Journal of Applied Polymer Science

Interfacial Modification of Single-Walled Carbon Nanotubes for High-Loading-Reinforced Polypropylene Composites

Siyang Liu, Zhe Wang, Guoming Lu, Yue Wang, Yue Zhang, Xiaodan He, Lixia Zhao, Zewen Li, Lichun Xuan, Dongyu Zhao

Key Laboratory of Chemical Engineering Process and Technology for High-Efficiency Conversion, College of Heilongjiang Province, School of Chemistry and Materials Science, Heilongjiang University, Harbin 150080, People's Republic of China

Correspondence to: Z. Wang (E-mail: zwangcn@gmail.com)

ABSTRACT: In this article, we present a strategy for fabricating polypropylene (PP)/polypropylene-regrafted single-walled carbon nanotube (PP-re-*g*-SWNT) composites with a high loading of single-walled carbon nanotubes (SWNTs; 20 wt %). The PP-re-*g*-SWNTs were characterized by X-ray photoelectron, Fourier transform infrared spectroscopy, transmission electron microscopy, and thermogravimetric analysis (TGA). The PP-re-*g*-SWNTs showed excellent interfacial adhesion and dispersion. Furthermore, PP molecules, about 72 wt % by mass, were homogeneously bonded onto the surface of the SWNTs according to TGA. In this hybrid nanocomposite system, the PP-re-*g*-SWNTs were covalently integrated into the PP matrix and became part of the conjugated network structure (as evidenced by differential scanning calorimetry and dynamic mechanical analysis) rather than just a separate component. Accordingly, the PP/PP-re-*g*-SWNT composites presented obvious improvements in mechanical properties and conductivity (from 10^{-10} to 10^{-2}). Most importantly, the tensile and flexural strength of the PP/PP-re-*g*-SWNT composites did not exhibit an obvious downturn with the addition of 20 wt % SWNTs; this was contrary to documented results. We believe that these new observations were due to the novel structure of the PP-re-*g*-SWNTs. © 2013 Wiley Periodicals, Inc. J. Appl. Polym. Sci. **2014**, *131*, 39817.

KEYWORDS: grafting; nanostructured polymers; structure–property relations

Received 9 April 2013; accepted 1 August 2013

DOI: 10.1002/app.39817

INTRODUCTION

Carbon nanotubes (CNTs) have been investigated over the past few years and have been found to hold promise for applications ranging from nanodevices to nanocomposites because of their remarkable electrical, mechanical, and thermal properties.[1–6] Among these applications, CNT-filled polymer composites are a large family and have been extensively studied. The first polymer nanocomposites using CNTs as fillers were reported in 1994 by Ajayan et al.[7] Since then, there have been many articles dedicated to improving the mechanical and electrical properties of polymer composites.[8–11] However, CNTs are normally curled and twisted, and therefore, individual CNTs embedded in a polymer only exhibit a fraction of their potential. One endeavor is to efficiently disperse individual nanotubes and establish strong chemical affinity, covalent or noncovalent, with the surrounding polymer matrix. In terms of the tensile modulus, it has been established by numerous studies that chemically modified nanotubes exhibit a significant increase in their modulus compared to the matrix resin. Micusik et al.[12] reported that polypropylene (PP) nanocomposites with multiwalled carbon nanotubes (MWCNTs) were produced by a small-scale masterbatch melt dilution technique. The Young's moduli of the composites were improved with an effective MWCNT content of 8 wt %, and the electrical conductivities of the composites reached 0.046 S/m with an effective MWCNTs content of 10 wt %. Kovalchuk et al.[13] reported that they synthesized PP/MWCNT composites via an *in situ* polymerization method. The tensile strength of the isotactic polypropylene (Ipp)/MWCNT was improved by 19.2% with a CNT loading of 0.5 wt %, and it began to decrease when the loading reached 3.5 wt %. Other similar results can be found in the literature.[14–30] To sum up, there usually exists a turning point where the tensile strength begins to decrease, and the value is around 10 wt %[31] for PP, whereas the polymer grafting does not exceed 40–50%.[32–34]

In this study, we prepared PP/PP-grafted single-walled carbon nanotube (SWNT) composites with PP containing 1 wt % maleic anhydride (MA; PP-*g*-MA) and amine-functionalized SWNTs. Different from reported methods,[35] the PP-*g*-SWNTs in this study were further grafted a second time with

ethanediamine treatment. The polymer-regrafted SWNTs filled with PP showed improved mechanical performance compared with the pure PP and PP reinforced with traditionally functionalized CNTs. We believe that the improvement was due to the covalent bonding of polymer chains to SWNTs, where strong chemical bonds and a conjugated network between the nanotubes and polymers were established. Moreover, the regrafted SWNTs had obvious effects[36] on the PP crystallinity and elevated electrical conductivity. This study provided a new path to make composites with specific loadings ranging from 0 to 20 wt % that were catered for tailored applications, such as conductive polymeric composites,[37] freestanding membranes,[38] polymer/SWNT composite films,[39–43] and so on.

EXPERIMENTAL

Materials

SWNTs (purity > 95%, diameter within 2 nm) produced by chemical vapor deposition were obtained from Shenzhen Nanotech Port Co., Ltd. (China). PP-*g*-MA (1 wt % MA) was prepared in this group. PP (type T30S) from PetroChina Daqing Petrochemical Co. was used as the matrix polymer. (3-Aminopropyl)-triethoxysilane (APTES) was purchased from the Chendu Organic Chemistry Institute.

Synthesis of the Polypropylene-Regrafted Single-Walled Carbon Nanotubes (PP-re-*g*-SWNTs)

The synthesis route for the PP-re-*g*-SWNTs is shown in Scheme 1. In a typical hydroxylation procedure, pristine SWNTs were added to a three-necked flask containing ethanol and KOH [1 g of SWNT, 10 g of KOH, and 400 mL of dimethylformamide (DMF)]. After ultrasonic dispersion for 30 min, the solution was refluxed for 10 h, and then the mixture was filtered by a membrane with a pore size of 0.45 μm and washed thoroughly with ethanol and deionized water three times. This was followed by drying at 80°C *in vacuo* for 12 h. The resulting product was designated as SWNT–OH. The amino-functionalization of the CNTs was carried out with an excess of APTES solution, which was added dropwise (0.5 g of SWNT–OH, 500 mL of DMF, and 8 mL of APTES), and the mixture was stirred at 80°C for 10 h; this enabled the reaction to go to completion. The mixture was then filtered by membranes with a pore size of 0.22 μm and washed thoroughly with DMF many times; this was followed by drying at 80°C *in vacuo* for 12 h. The resulting product was designated as SWNT–NH_2.[44]

PP-*g*-MA and SWNT–NH_2 were blended in a mixer at a speed of 80 rpm at 120°C with a weight ratio of 2:1 to ensure the complete conversion of amine groups to imide groups. The product was named PP-*g*-SWNT after filtration with a 0.22-μm membrane and vacuum drying at 80°C for 12 h. The prepared PP-*g*-SWNTs were separated and purified by repeated hot-vacuum filtration at about 120°C to remove the unreacted PP and any other soluble byproducts. In the following step, ethanediamine was added to a three-necked flask containing melted PP-*g*-SWNTs. After ultrasonic dispersion for 30 min, the solution was refluxed for 36 h, and then the mixture was filtered and dried at 80°C *in vacuo* for 12 h. The yield was designated as PP-*g*-SWNT–NH_2. Finally, PP–MA was added to SWNT–PP–NH_2 with weight ratio of 2:1 to ensure the complete reaction, and this resulted in the PP-re-*g*-SWNTs.

PP/PP-re-*g*-SWNT Composite Preparation

PP-re-*g*-SWNTs were used as a masterbatch to blend with PP to obtain composites with different SWNT contents. The blending was carried out in hot xylene at 120°C for 30 min, and then the mixture was filtered and dried at 80°C *in vacuo* for 12 h. We used the mold that we made by ourselves to melt blend powder and fabricate the composites by exerting pressure. The composites were then pressed into a sheet (first at 180°C and then at room temperature) with diameters of 5 and 2.5 mm to perform mechanical tests.

Characterization

The PP-re-*g*-SWNTs were characterized by X-ray photoelectron spectroscopy (XPS) with a Kratos-AXIS ULTRA DLD with an Al Kα X-ray source. In curve fitting, the widths of the Gaussian peaks were kept constant in a particular spectrum. Fourier transform infrared (FTIR) spectra were recorded on a PerkinElmer Spectrum model 100 FTIR spectrometer. Transmission electron microscopy (TEM) micrographs of SWNTs and PP-re-*g*-SWNTs were obtained with a JEM-2100(200 kV). Differential scanning calorimetry analyses were performed on a PerkinElmer Pyris instrument. Each sample was heated to 220°C at a heating rate of 10°C/min after holding at 220°C for 10 min; the sample was then cooled to 0°C at a cooling rate of 10°C/min in a nitrogen atmosphere. Dynamic mechanical data were collected at a frequency of 1 Hz and at a heating rate of 5°C/min within the temperature range from 20 to 160°C in a nitrogen atmosphere with a DMS 6100 in stretching mode. Samples with dimensions of 50 × 5 × 2.5 mm^3 were used. The tensile properties of the composites were measured at room temperature with an R-9100 mechanical tester from Shen Zhen Rerer Instrument Co., Ltd. The strain rate was 5 mm/min with a load of 1 kN. The flexural properties of the composites were measured with an HY-1080 mechanical tester from Shanghai Heng Yi Precision Instrument Co., Ltd. The electrical conductivity was measured by a ZC36 megger from Shanghai No. 6 Electricity Meter Co., Ltd.

RESULTS AND DISCUSSION

Grafting of PP onto the SWNTs

The XPS spectra for the pristine CNTs, CNT–OH, CNT–NH_2, PP-*g*-SWNTs, and PP-re-*g*-SWNTs and the C1s spectra for SWNT–OH, PP-*g*-SWNTs, and PP-re-*g*-SWNTs are shown in Figure 1. The chemical compositions are listed in Table I. For the pristine SWNTs, aside from the main C—C peak at 284.5 eV, a weak O1s peak at 533.5 eV (O 1s, atom %: 2.81) was attributed to atmospheric moisture or oxidation during the purification process.[39] For the SWNT–OH sample, the concentration of oxygen increased up to 4.19 atom %, and the O1s spectrum showed a binding energy (BE) of 531.3 eV, which was assigned to C–OH; this implied that the SWNTs were successfully hydroxylated. In comparison with the SWNT–OH, two new photoemission peaks, with BEs of 102.5 eV (Si2p: 0.58 atom %) and 399.1 eV (N1s: 1.37atom %), appeared in the XPS spectrum of the SWNT–NH_2. The higher surface oxygen content (4.54 atom %) was attributed to the hydrolysis of

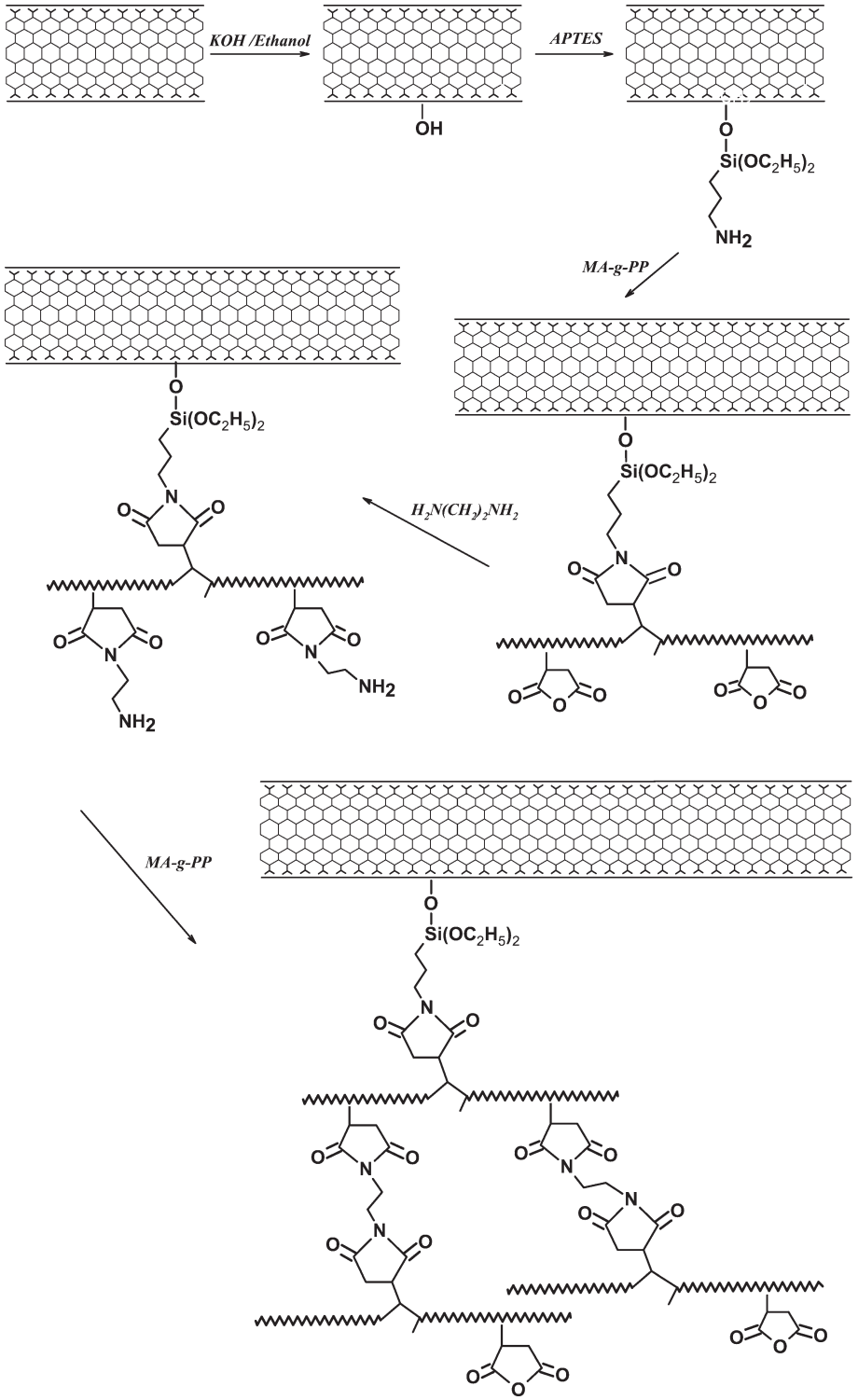

Scheme 1. Schematic synthesis route for PP-re-*g*-SWNTs.

APTES[44] and provided the proof for the amino functionalization of the SWNTs. Notably, the carbon percentage increased to 97.16 atom % for the PP-*g*-SWNT sample and 97.29 atom % for the PP-re-*g*-SWNT sample. This was due to the introduction of PP molecules onto the surface of the SWNTs. From the thermogravimetric analysis (TGA) data, about 70 wt % of the PP molecules were attached onto the surface of the SWNTs by mass. More proof of PP attachment was the splitting of the C1s peak [Figure 1(b,c)], namely, from one photoemission peak for the SWNT–OH, PP-*g*-SWNTs, and PP-re-*g*-SWNTs to several peaks. The PP-*g*-SWNT and PP-re-*g*-SWNT samples could be attributed to five peaks, which were the graphite signal, carbon

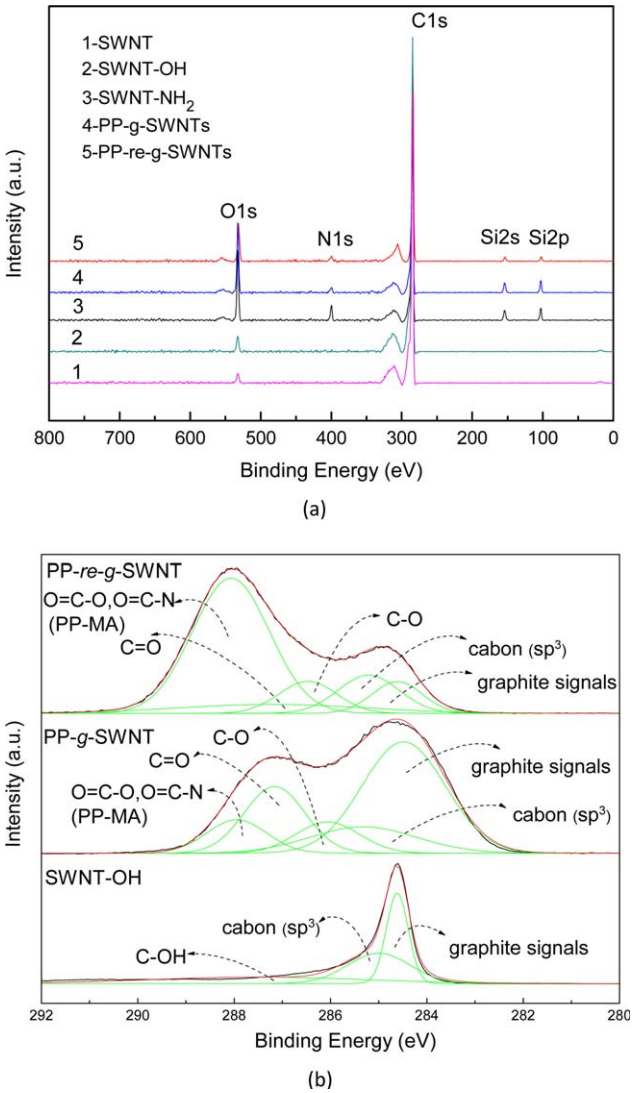

Figure 1. (a) XPS wide spectra of the pristine SWNTs, SWNT–OH, SWNT–NH_2, PP-*g*-SWNT, and PP-re-*g*-SWNTs samples and (b) C1s XPS spectra of SWNT–OH, PP-*g*-SWNT, and PP-re-*g*-SWNTs samples. [Color figure can be viewed in the online issue, which is available at wileyonlinelibrary.com.]

sp^3, C—O, C═O, O═C—O, and O═—C—N (PP-*g*-MA). Finally, we safely concluded that PP was successfully grafted onto the surface of the SWNTs.

Table I. Atomic Percentages by XPS

Sample	C (atom %)	N (atom %)	O (atom %)	Si (atom %)
SWNT	97.2	NA	2.8	NA
SWNT-OH	95.8	NA	4.1	NA
SWNT-NH_2	93.5	1.4	4.5	0.5
PP-*g*-SWNTs	97.1	0.5	1.7	0.5
PP-re-*g*-SWNTs	97.3	0.6	1.8	0.2

NA = not applicable.

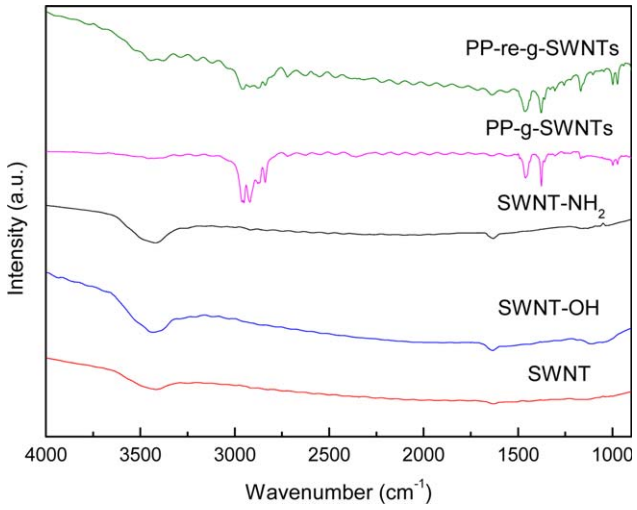

Figure 2. FTIR spectra of the pristine SWNTs, SWNT–OH, SWNT–NH_2, PP-*g*-SWNT, and PP-re-*g*-SWNTs. [Color figure can be viewed in the online issue, which is available at wileyonlinelibrary.com.]

Figure 2 shows the IR spectra for the pristine SWNTs and modified SWNTs. The appearance of a rather weak and broad absorption band at 3445 cm^{-1} was due to the presence of —OH groups on the surface of the pristine SWNTs; this resulted from either ambient atmospheric moisture bound to the CNTs or oxidation during the purification of the raw SWNTs. The peak at 1630 cm^{-1} was ascribed to the stretching of the C═C groups only for the SWNTs. In the IR spectrum of SWNT–OH, a strong and broad band at 3400–3500 cm^{-1} was assigned to the —OH groups which arose from the hydroxylation of the SWNTs, and the peaks at 1115 and 1030 cm^{-1} were attributed to the bending vibration of O—H and the stretching of C—O, respectively. For the IR spectrum of SWNT–NH_2, the diminished peak at 3400–3520 cm^{-1} indicated largely decreased OH groups, and the peak at 1152 cm^{-1} was attributed to the stretching of the Si—O—Si groups. The previous changes in the absorption peaks and bands proved the occurrence of the amino functionalization of the CNTs. As for the PP-*g*-SWNTs and PP-re-*g*-SWNTs, the two new absorption peaks at 2853 and 2922 cm^{-1} were assignable to the characteristic peaks of PP. In addition, 1475 and 1386 cm^{-1} were assignable to the stretching of the C—N and N—H groups from amide and imide, respectively. The previous changes verified the presence of the PP moieties on the surface of the SWNTs.

Figure 3 presents the TEM images of the pristine SWNTs, PP-*g*-SWNTs, and PP-re-*g*-SWNTs. The surface of the control SWNT sample [Figure 3(b,c)] was quite clean; this indicated that the most PP physically adsorbed on the surface of SWNTs could be removed by sufficient hot-vacuum filtration. We observed that the diameter of the raw SWNTs [Figure 3(a)] was around 2 nm, whereas the PP-*g*-SWNTs and PP-re-*g*-SWNTs [Figure 3(b,c)] were much thicker because of the polymer wrapping. The thickness of the PP-*g*-SWNTs and PP-re-*g*-SWNTs were 8 and 40 nm, respectively. Using these XPS analyses, we were able to draw the conclusion that the layer was the product of PP. This suggested that the grafting ratio of the PP-re-*g*-SWNTs was

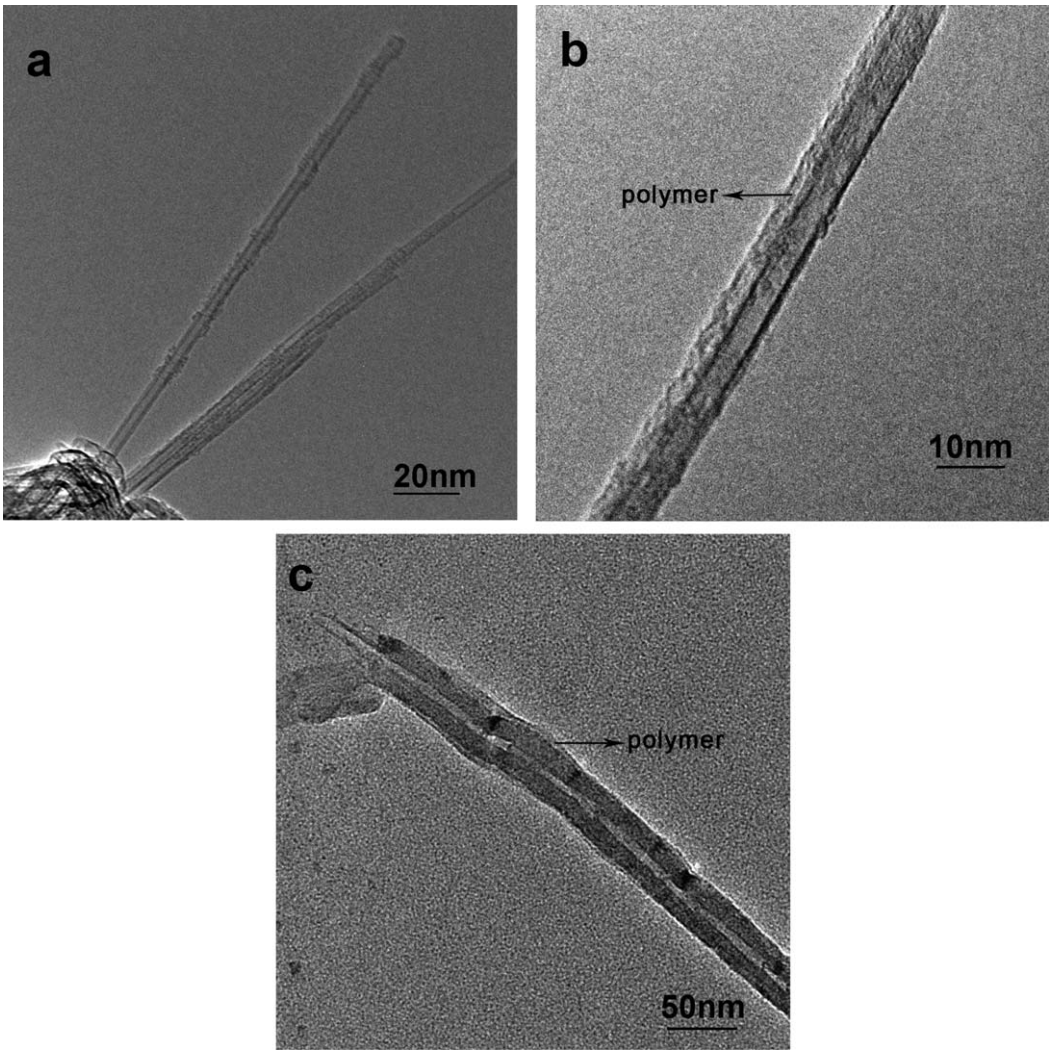

Figure 3. TEM micrographs of the (a) pristine SWNT, (b) PP-*g*-SWNTs showing nanotubes covered by polymer, and (c) PP-re-*g*-SWNTs showing nanotubes covered by more polymer.

much higher than that of the PP-*g*-SWNTs, which could be proven by TGA. As shown in Figure 4, there was an obvious two-step decomposition for the PP-*g*-SWNTs and PP-re-*g*-SWNTs; these were PP decomposition and SWNT decomposition according to the curves of the PP-*g*-MA and SWNTs. The grafting ratio of the PP-*g*-SWNTs and PP-re-*g*-SWNTs were calculated to be about 20 and 72 wt %, respectively.

Mechanical and Electrical Properties of the Composites

The mechanical properties of the PP/PP-*g*-SWNTs and PP/PP-re-*g*-SWNTs composite and the tensile and flexural properties are shown in Figure 5. The tensile strength and flexural strength of the PP/PP-re-*g*-SWNTs with 0.6 wt % SWNT loadings were increased by maxima of 55.2 and 66%, respectively, compared to the PP/PP-*g*-SWNT composites (maximum increments = 47.1 and 53.8%). Unexpectedly, the tensile strength and flexural strength of the PP/PP-re-*g*-SWNTs composite with 20 wt % SWNT loadings did not decrease that contrary to literature. In fact, they were still improved by 5.0 and 1.7%. The improved

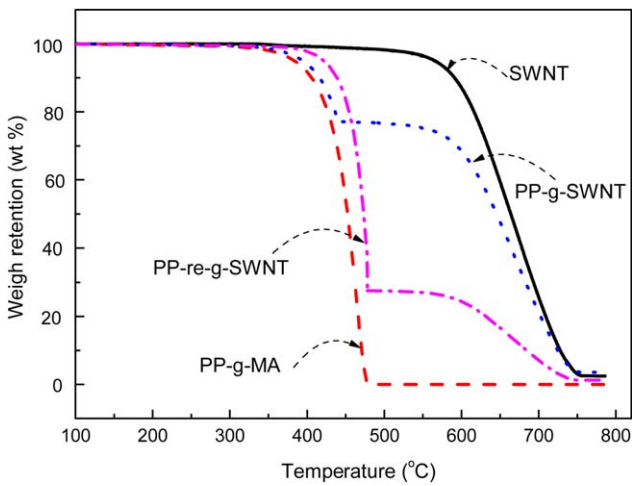

Figure 4. TGA curves of the SWNTs, PP-*g*-SWNTs, PP-re-*g*-SWNTs, and PP-*g*-MA. [Color figure can be viewed in the online issue, which is available at wileyonlinelibrary.com.]

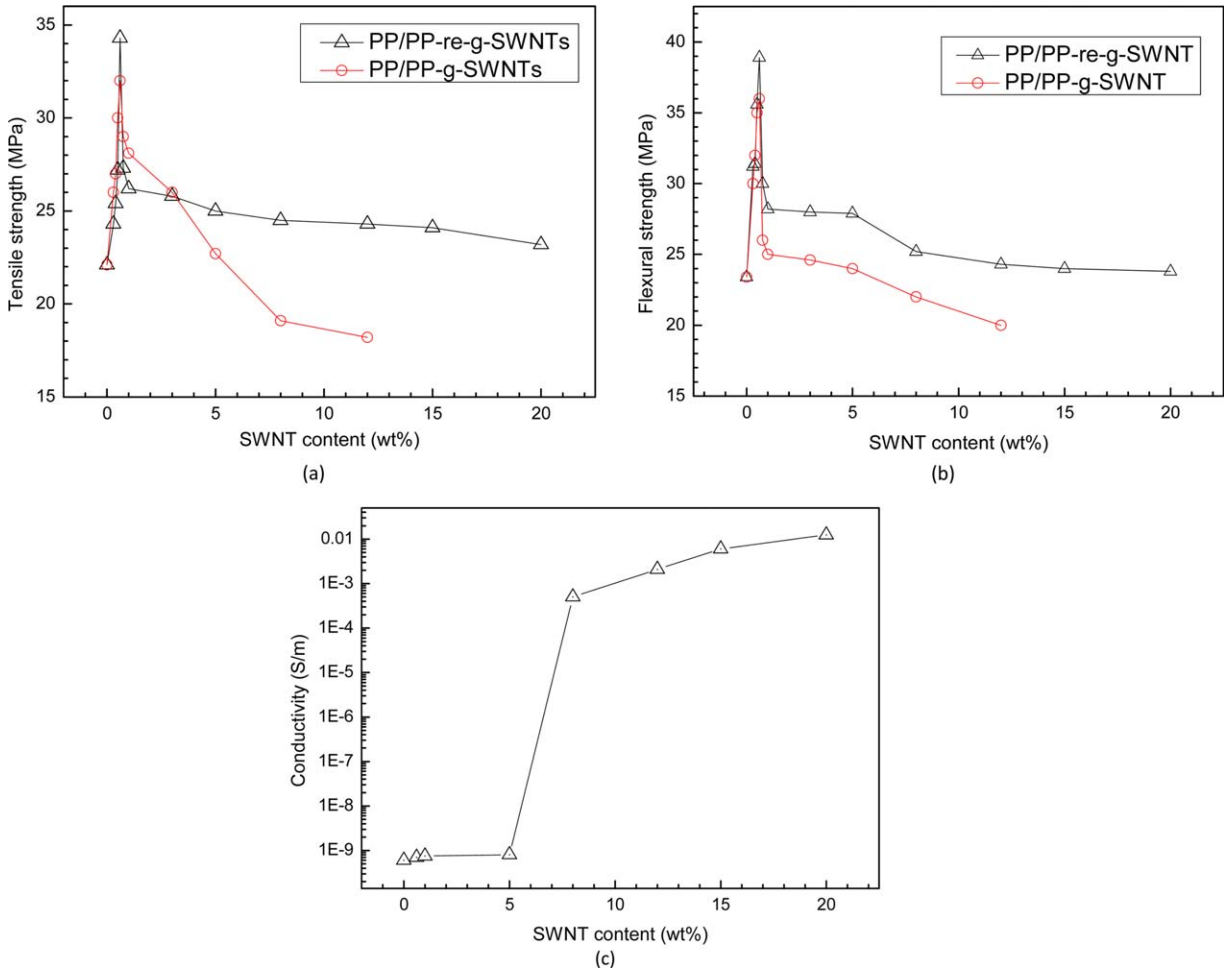

Figure 5. (a) Tensile strength and (b) flexural strength curves of PP-*g*-SWNT- and PP-re-*g*-SWNT-reinforced PP matrix composites and (c) electrical conductivity curve of the PP/PP-re-*g*-SWNTs composites. [Color figure can be viewed in the online issue, which is available at wileyonlinelibrary.com.]

mechanical properties of the PP/PP-re-*g*-SWNTs composite were due to the covalent chemical bonding of the polymer chains to the SWNTs, where much stronger chemical bonds and conjugated network between the nanotubes and polymers were established. As a result, the stronger interfacial adhesion developed a better dispersion system between the PP and SWNTs.

Differential scanning calorimetry analysis was performed, and in summary, the melting temperature, crystallinity temperature, and crystallinity increased progressively upon the addition of the PP-re-*g*-SWNTs. The results indicate that the PP/PP-re-*g*-SWNTs promoted the crystallinity of PP (Table II). In other words, the PP and PP-re-*g*-SWNTs had a strong nucleation effect on the crystallinity of the polymer; this reduced the defects of interaction in the composites. Moreover, the dynamic mechanical analysis data suggested that the loss modulus of the PP/PP-re-*g*-SWNTs composites increased progressively upon the addition of the PP-re-*g*-SWNTs; this may have been related to the cohesive interactions between the large surface area of the nanotubes and the PP components.[45] The electrical properties of the PP/PP-re-*g*-SWNTs composites and PP are shown in Figure 5(c). The electrical conductivity increased with increasing SWNT content. Therefore, the polymer composites experienced a transition from electrical insulator to conductor. Furthermore, the better interfacial adhesion between the SWCNTs and the PP matrix generated an additional electrical pathway.[46]

Table II. Melting and Crystallization Parameters of the PP and PP-re-*g*-SWNT/PP Composites

Sample	T_m (°C)[a]	T_c (°C)[b]	ΔH_m (J/g)[c]	X_c (%)[d]
PP	131	110	77	36
PP-re-*g*-SWNT (0.3%)/PP	132	111	80	39
PP-re-*g*-SWNT (0.6%)/PP	132	112	88	42
PP-re-*g*-SWNT (1%)/PP	133	113	89	43
PP-re-*g*-SWNT (5%)/PP	133	114	90	43
PP-re-*g*-SWNT (12%)/PP	136	115	91	44

[a] Melting temperature.
[b] Crystallinity temperature.
[c] Enthalpy.
[d] Crystallinity.

CONCLUSIONS

The SWNTs were dispersed well in the PP matrix and developed excellent interfacial adhesion because of the novel structure of the PP-re-*g*-SWNTs, as characterized by XPS, IR, and TEM. The tensile strength, flexural strength, electrical conductivity, loss modulus, and crystallinity were all improved upon the addition of the PP-re-*g*-SWNTs. On the other hand, the mechanical performance still held with ultrahigh CNT loadings (20 wt %); this is a new finding in composite science and is promising for both practical applications and academia.

ACKNOWLEDGMENTS

The authors gratefully acknowledge the financial support of the National Natural Science Foundation of China (contract grant number 31270608) and the Heilongjiang Educational Committee (contract grant number 1511385).

REFERENCES

1. Ajayan, P. M.; Stephan, O.; Colliex, C.; Trauth, D. *Science* **1994**, *265*, 1212.
2. Moniruzzaman, M.; Winey, K. I. *Macromolecules* **2006**, *39*, 5194.
3. Sandler, J.; Shaffer, M. S. P.; Prasse, T.; Bauhofer, W.; Schulte, K.; Windle, A. H. *Polymer* **1999**, *40*, 5967.
4. Gong, X. Y.; Liu, J.; Baskaran, S.; Voise, R. D.; Young, J. S. *Chem. Mater.* **2000**, *12*, 1049.
5. Mincheva, R.; Meyer, F.; Verge, P.; Raquez, J.-M. *Macromol. Rapid Commun.* **2011**, *32*, 1960.
6. Li, Y.; Zhao, L.; Shimizu, H. *Macromol. Rapid Commun.* **2011**, *32*, 289.
7. Ajayan, P. M.; Stephan, O.; Colliex, C.; Trauth, D. *Science* **1994**, *265*, 1212.
8. McIntosh, D.; Khabashesku, V. N.; Barrera, E. V. *Chem. Mater.* **2006**, *18*, 4561.
9. Yang, B.-X.; Shi, J.-H.; Pramod, K. P.; Goh, S. H. *Compos. Sci. Technol.* **2008**, *68*, 2490.
10. Kearns, J. C.; Shambaugh, R. L. *J. Appl. Polym. Sci.* **2002**, *86*, 2079.
11. Haggenmueller, R.; Gommans, H. H.; Rinzler, A. G.; Fischer, J. E.; Winey, K. I. *Chem. Phys. Lett.* **2000**, *330*, 219.
12. Micusik, M.; Omastova, M.; Krupa, I.; Prokes, J.; Pissis, P.; Logakis, E.; Pandis, C.; Potschke, P.; Pionteck, J. *J. Appl. Polym. Sci.* **2009**, *113*, 2536.
13. Kovalchuk, A. A.; Shevchenko, V. G.; Shchegolikhin, A. N.; Nedorezova, P. M.; Klyamkina, A. N.; Aladyshev, A. M. *Macromolecules* **2008**, *41*, 7536.
14. Zhou, Z.; Wang, S.; Lu, L.; Zhang, Y.; Zhang, Y. *Compos. Sci. Technol.* **2008**, *68*, 1727.
15. Masuda, J.; Torkelson, J. M. *Macromolecules* **2008**, *41*, 5974.
16. Andrews, R.; Jacques, D.; Rao, A. M.; Rantell, T.; Derbyshire, F.; Chen, Y. *Appl. Phys. Lett.* **1999**, *75*, 1329.
17. Chen, J.; Ramasubramaniam, R.; Xue, C.; Liu, H. *Adv. Funct. Mater.* **2006**, *16*, 114.
18. Du, F.; Fischer, J. E.; Winey, K. I. *J. Polym. Sci. Part B: Polym. Phys.* **2003**, *41*, 3333.
19. Gorga, R. E.; Cohen, R. E. *J. Polym. Sci. Part B: Polym. Phys.* **2004**, *42*, 2690.
20. Sabba, Y.; Thomas, E. L. *Macromolecules* **2004**, *37*, 4815.
21. Liu, L.; Eder, M.; Burgert, I.; Tasis, D.; Prato, M.; Wagner, H. D. *Appl. Phys. Lett.* **2007**, *90*, 083108.
22. Mamedov, A. A.; Kotov, N.; Prato, M.; Guldi, D. M.; Wicksted, J. P.; Hirsch, A. *Nat. Mater.* **2002**, *1*, 190.
23. Haggenmueller, R.; Gommans, H. H.; Rinzler, A. G.; Fischer, J. E.; Winey, I. *Chem. Phys. Lett.* **2000**, *330*, 219.
24. Jia, Z.; Wang, Z.; Xu, C.; Liang, J.; Wei, B.; Wu, D. *Mater. Sci. Eng. A* **1999**, *271*, 395.
25. Olek, M.; Ostrander, J.; Jurga, S.; Mohvald, H.; Kotov, N.; Kempa, K. *Nano Lett.* **2004**, *4*, 1889.
26. Shofner, M. L.; Rodriguez-Macias, F. J.; Vaidyanathan, R.; Barrera, E. V. *Compos. A* **2003**, *34*, 1207.
27. Li, Y.; Shimizu, H. *Polymer* **2007**, *48*, 2203.
28. Peeterbroeck, S.; Alexandre, M.; Nagy, J. B.; Pirlot, C.; Fonseca, A.; Moreau, N. *Compos. Sci. Technol.* **2004**, *64*, 2317.
29. Xia, H.; Wang, Q.; Qiu, G. *Chem. Mater.* **2003**, *15*, 3879.
30. Bokobza, L. *Mech. Vibr. Spectrosc.* **2009**, *51*, 52.
31. Spitalskya, Z.; Tasisb, D.; Papagelisb, K.; Galiotisa, C. *Prog. Polym. Sci.* **2010**, *35*, 357.
32. Czerw, R.; Guo, Z.; Ajayan, P. M.; Sun, Y. P.; Carroll, D. L. *Nano Lett.* **2001**, *1*, 423.
33. Hu, H.; Ni, N.; Mandal, S. K.; Montana, V.; Zhao, B.; Haddon, R. C. *J. Phys. Chem. B* **2005**, *109*, 4285.
34. Ge, J. J.; Zhang, D.; Li, Q.; Hou, H.; Graham, M. J.; Dai, L. *J. Am. Chem. Soc.* **2005**, *127*, 9984.
35. Yang, B.-X.; Shi, J.-H.; Pramod, K. P.; Goh, S. H. *Compos. Sci. Technol.* **2008**, *68*, 2490.
36. Li, L.; Li, B.; Hood, M. A.; Li, C. Y. *Polymer* **2009**, *50*, 953.
37. Frank, S.; Poncharal, P.; Wang, Z. L.; de Heer, W. A. *Science* **1998**, *280*, 1744.
38. Mamedov, A. A.; Kotov, N. *Nat. Mater.* **2002**, *1*, 190.
39. Zhang, X.; Liu, T.; Sreekumar, T. V. *Am. Chem. Soc.* **2003**, *3*, 1286.
40. Spitalskya, Z.; Tasisb, D.; Papagelisb, K.; Galiotisa, C. *Prog. Polym. Sci.* **2010**, *35*, 357.
41. Potschke, P.; Zschoerper, N. P.; Moller, B. P.; Vohrer, U. *Macromol. Rapid Commun.* **2009**, *30*, 1828.
42. Park, S. J.; Cho, M. S.; Lim, S. T.; Choi, H. J.; Jhon, M. S. *Macromol. Rapid Commun.* **2003**, *24*, 1070.
43. Minus, M. L.; Chae, H. G.; Kumar, S. *Macromol. Rapid Commun.* **2010**, *31*, 310.
44. Song, P.; Shen, Y.; Du, B.; Guo, Z.; Fang, Z. *Nanoscale* **2009**, *1*, 118.
45. Kotsilkova, R.; Ivanov, E.; Krusteva, E.; Silvestre, C.; Cimmino, S.; Duraccio, D. *J. Appl. Polym. Sci.* **2010**, *115*, 3576.
46. Lee, S. J.; Cho, E.; Jeon, S. H.; Youn, J. R. *Carbon* **2007**, *45*, 2810.